Animal Nutrition 16 (2024) 443–456

Contents lists available at ScienceDirect

Animal Nutrition

journal homepage: http://www.keaipublishing.com/en/journals/aninu/

Original Research Article

Dietary sodium acetate and sodium butyrate attenuate intestinal damage and improve lipid metabolism in juvenile largemouth bass (*Micropterus salmoides*) fed a high carbohydrate diet by reducing endoplasmic reticulum stress

Liulan Zhao [1], Liangshun Cheng [1], Yifang Hu [1], Xiaohui Li, Yihui Yang, Jin Mu, Lianfeng Shen, Guojun Hu, Kuo He, Haoxiao Yan, Qiao Liu*, Song Yang*

College of Animal Science and Technology, Sichuan Agricultural University, Chengdu, Sichuan, 611130, China

ARTICLE INFO

Article history:
Received 29 June 2023
Received in revised form
11 December 2023
Accepted 14 December 2023
Available online 20 December 2023

Keywords:
Sodium acetate
Sodium butyrate
High carbohydrate diet
Endoplasmic reticulum stress
Intestine health
Lipid metabolism

ABSTRACT

High-carbohydrate (HC) diets decrease the intestinal levels of sodium acetate (SA) and sodium butyrate (SB) and impair the gut health of largemouth bass; however, SA and SB have been shown to enhance immunity and improve intestinal health in farmed animals. Thus, the present study was to investigate the effects of dietary SA and SB on HC diet-induced intestinal injury and the potential mechanisms in juvenile largemouth bass. The experiment set five isonitrogenous and isolipidic diets, including a low-carbohydrate diet (9% starch) (LC), a high carbohydrate diet (18% starch) (HC), and the HC diet supplemented with 2 g/kg SA (HCSA), 2 g/kg SB (HCSB) or a combination of 1 g/kg SA and 1 g/kg SB (HCSASB). The feeding experiment was conducted for 8 weeks. A total of 525 juvenile largemouth bass with an initial body weight of 7.00 ± 0.20 g were used. The results showed that dietary SA and SB improved the weight gain rate and specific growth rate ($P < 0.05$) and ameliorated serum parameters (alkaline phosphatase, acid phosphatase, glutamate transaminase, and glutamic oxaloacetic transaminase) ($P < 0.05$). And, importantly, dietary SA and SB repaired the intestinal barrier by increasing the expression levels of zonula occludens-1, occludin, and claudin-7 ($P < 0.05$), reduced HC-induced intestinal damage, and alleviated intestinal inflammation and cell apoptosis by attenuating HC-induced intestinal endoplasmic reticulum stress ($P < 0.05$). Further results revealed that dietary SA and SB reduced HC-induced intestinal fat deposition by inhibiting adipogenesis and promoting lipolysis ($P < 0.05$). In summary, this study demonstrated that dietary SA and SB attenuated HC-induced intestinal damage and reduced excessive intestinal fat deposition in largemouth bass.

1. Introduction

As aquaculture is rapidly developing and fish meal prices are increasing, there is a growing interest in producing affordable aquafeeds (Wang et al., 2015). Including high-value nutrients such as carbohydrates and lipids in the feed is a possible strategy for enhancing the protein-sparing effect of aquafeed. Carbohydrates are much less expensive than lipids, and a moderate amount of carbohydrates may improve economic benefits and decrease water pollution (Ali and Jauncey, 2004; Sankian et al., 2017). However, a high-carbohydrate (HC) diet can lead to impaired gut health, especially in carnivorous fish (Ding et al., 2020; Pan et al., 2022; Shi et al., 2022a). In largemouth bass, previous research has suggested that HC can disrupt the gut microbial balance, decrease the concentrations of short-chain fatty acids (acetate and butyrate), and impair gut health (Zhou et al., 2021).

* Corresponding authors.
E-mail addresses: 14493@sicau.edu.cn (Q. Liu), yangsong@sicau.edu.cn (S. Yang).
[1] These authors contributed equally to this work.
Peer review under responsibility of Chinese Association of Animal Science and Veterinary Medicine.

Production and Hosting by Elsevier on behalf of KeAi

https://doi.org/10.1016/j.aninu.2023.12.002

The gut is a vital digestive and immune organ that acts as a vital barrier to prevent toxins and pathogens from entering the body (Kumar et al., 2005). It is noteworthy that dietary factors are the primary cause of intestinal dysfunction (Bibbò et al., 2016; Díez-Sainz et al., 2021; Wan et al., 2019). Studies have reported that intake of 17% carbohydrate induced intestinal endoplasmic reticulum stress (ERS) in largemouth bass that in turn promoted inflammation and apoptosis (Zhao et al., 2021c). High carbohydrate diets also led to lipid deposition and oxidative stress in intestinal epithelial cells (Wu et al., 2022; Zhao et al., 2020a). Interestingly, short-chain fatty acids (acetate, propionate, and butyrate) produced by microorganisms in the gut through metabolizing undigested fiber or carbohydrates have been demonstrated to regulate human, mammalian, and fish microbiota and improve gut health (McCarville et al., 2020). For example, supplementing the diet with 1 g/kg of sodium acetate (SA) can improve the microbial community structure and regulate the intestinal lipid distribution to promote intestinal health (Xun et al., 2023). In addition, supplementing the diet with acetate-forming bacteria or 1.85 g/kg of SA alleviated HC-induced metabolic disorders and intestinal inflammation and thereby improved the growth of Nile tilapia (Li et al., 2020a; Xu et al., 2022c). Similarly, supplementation with 2 g/kg of sodium butyrate (SB) improved the growth and intestinal immune function of grass carp as well as the liver function of largemouth bass fed a high-fat diet (Chen et al., 2022; Tian et al., 2017). Therefore, SA and SB may be potential supplements that can alleviate HC-induced gut health and metabolic disturbances in fish, and thus, supplementing the diet with SA and SB was set at 2 g/kg in this experiment. However, whether SA and SB can reduce HC-induced intestinal damage in juvenile largemouth bass remains to be further investigated.

Largemouth bass has become one of the most important species of farmed fish due to its tasty meat, rapid growth, and high market potential (Fan et al., 2022). Like most carnivorous fish, largemouth bass has a limited capacity for carbohydrate utilization (Li et al., 2020). Previous research has indicated that starch levels of 7% to 12% had no harmful effects on largemouth bass, whereas starch levels of 17% and above impaired gut health, disrupted the balance of the intestinal microbiota, and decreased intestinal acetate and butyrate levels (Huang et al., 2021; Zhao et al., 2022a). Hence, the purpose of this study was to assess whether the exogenous supplementation of SA and SB could ameliorate the negative effects on growth performance, intestinal health, and lipid metabolism in largemouth bass fed a HC diet. Other objectives of this study are to identify the mechanisms that may be involved and to provide a theoretical basis for the application of SA and SB.

2. Materials and methods

2.1. Animal ethics

The experiment was completed under the supervision of the Animal Care Advisory Committee of Sichuan Agricultural University (No. 2021202068). All experimental animals and animal management were approved by the China Animal Care Committee (No. 2020-AFFRI-CAAS-001). The experiment complied with the ARRIVE guidelines.

2.2. Experimental diets

Sodium acetate and SB (purity $\geq$ 98%) were obtained from Xinao Agriculture and Animal Husbandry Development Co., Ltd (Xiamen, Fujian, China). Five isonitrogenous (44% crude protein) and isolipidic (10% crude lipid) experimental diets were made (Table 1) (Zhao et al., 2022a), including a low carbohydrate diet (9% starch; LC), a high carbohydrate diet (18% starch; HC) and a high carbohydrate diet with supplemented 2 g/kg SA (HCSA), 2 g/kg SB (HCSB), and a combination of 1 g/kg SA and 1 g/kg SB (HCSASB). The added levels of SA and SB referred to previous studies (Chen et al., 2023; Zhou et al., 2023). The feed ingredients were crushed and sieved through 80 mesh. After the dry ingredients were thoroughly mixed, oil and water were added. Pellets of 3 mm and 4 mm diameter were produced using a pelletiser. The pellets were dried with a fan and store at −20 °C until use.

Standard methods were used to measure the chemical composition of the diet (AOAC, 2005). Crude protein content was analyzed according to the Kjeldahl method (Kjeltec 2300, FOSS, Hilleroed, Denmark). Crude lipid content was measured by petroleum ether extraction (Soxtec 2055, FOSS, Denmark). Moisture content was determined using a vacuum freeze dryer (GZX-9240MBE, Shanghai, China). Ash content was determined by burning at high temperature in a muffle furnace.

2.3. Fish and feeding trial

Largemouth bass were obtained from a farm (Qionglai Hongbo Agricultural Co., Ltd., China). The fish were kept temporarily in an indoor tank for two weeks and fed a LC diet twice daily. A total of

Table 1
Formulation and chemical composition of the diets[1] (% dry matter).

Ingredients	LC	HC	HCSA	HCSB	HCSASB
Fish meal[2]	51	51	51	51	51
Soybean oil[2]	6	6	6	6	6
Wheat gluten meal[2]	4	4	4	4	4
Extruded-soybean[2]	3	3	3	3	3
Spray dried plasma protein powder[2]	5	5	5	5	5
α-Starch[2]	9	18	18	18	18
Soy protein concentrate[2]	4.5	4.5	4.5	4.5	4.5
Microcrystalline cellulose[2]	12.5	3.5	3.3	3.3	3.3
$Ca(H_2PO_4)_2$[2]	1.5	1.5	1.5	1.5	1.5
Choline chloride[2]	0.5	0.5	0.5	0.5	0.5
Yeast hydrolyzate[2]	1	1	1	1	1
Vitamin premix[3]	1	1	1	1	1
Mineral premix[4]	1	1	1	1	1
SA[5]	0.0	0.0	0.2	0.0	0.1
SB[5]	0.0	0.0	0.0	0.2	0.1
Chemical composition					
Crude protein[6]	44.57	44.60	44.18	44.35	44.70
Crude lipid[6]	10.40	10.29	10.42	10.24	10.52
Moisture[6]	8.68	8.58	8.70	8.89	8.75
Ash[6]	12.56	12.49	12.41	12.26	12.10
Crude fiber[6]	7.60	1.31	1.45	1.56	1.48
Nitrogen-free extract[7]	16.19	22.73	22.84	22.70	22.45
Carbohydrate[8]	23.79	24.04	24.29	24.26	23.93
Gross energy[9], kJ/g dry matter	18.71	18.73	18.72	18.68	18.82

SA = sodium acetate; SB = sodium butyrate.

[1] LC represents a low carbohydrate diet; HC represents a high carbohydrate diet; HCSA, HCSB, and HCSASB represent a high carbohydrate diet supplemented with 2 g/kg SA, 2 g/kg SB, and a combination of 1 g/kg SA and 1 g/kg SB, respectively.

[2] Supplied by Chengdu Sanwang farming Co., Ltd. (China).

[3] Vitamin premix provided the following (mg/kg diet): vitamin A, 16,000 IU; vitamin D_3, 8,000 IU; vitamin K_3, 14.72; vitamin B_1, 17.80; vitamin B_2, 48; vitamin B_6, 29.52; vitaminB_{12}, 0.24; vitamin E, 160; vitamin C, 800; niacinamide, 79.20; calcium-pantothenate, 73.60; folic acid, 6.40; biotin, 0.64; inositol, 320; choline chloride, 1,500; L-carnitine, 100.

[4] Mineral premix provided the following (mg/kg diet): Cu ($CuSO_4$), 2.00; Zn ($ZnSO_4$), 34.4; Mn ($MnSO_4$), 6.20; Fe ($FeSO_4$), 21.10; I ($Ca(IO_3)_2$), 1.63; Se (Na_2SeO_3), 0.18; Co ($COCl_2$), 0.24; Mg ($MgSO_4 \cdot H_2O$), 52.70.

[5] Supplied by Xinao Agriculture and Animal Husbandry Development Co., Ltd. (China).

[6] Crude protein, crude lipid, ash, crude fiber and moisture contents were measured value.

[7] Nitrogen-free extract = 100 − (moisture + crude protein + crude lipid + ash + crude fiber).

[8] Carbohydrate = nitrogen-free extract + crude fiber.

[9] Gross energy was calculated by NRC (2011) contents.

525 fish (initial body weight of 7.00 ± 0.20 g) were distributed in 15 white cylindrical tanks (35 fish per tank), with 5 treatments per tank and 3 replicates per treatment. The tanks were with 1 m of diameter and held 300 L of water. The fish were fed the trial diets twice daily (08:00 and 16:00) until visual satiety over a period of 8 weeks. During feeding, the water temperature was kept at 25.0 ± 2.0 °C, the dissolved oxygen level was maintained above 6.5 mg/L, the pH was at 6.2 to 7.2, and the NH_4^+-N level was lower than 0.2 mg/L. We siphoned off the remaining faeces and replenished around 2/5 of the water after every feeding to maintain a clean environment. The photoperiod was kept natural throughout the experiment (12 h light:12 h dark).

2.4. Sample collection

After completing the feeding trial, the fish were fasted for 24 h and then anaesthetized with 0.1 g/L MS-222 (Sigma, St Louis, MO, USA). Blood was obtained from the tail vein using a heparinized syringe and then centrifuged at 2,500 × *g* for 10 min at 4 °C. The fish were dissected to remove the intestinal contents, and the midgut of fish was immobilized in 4% paraformaldehyde ($n = 3$) for histological observation. A portion of the midgut ($n = 3$) was immediately post-fixed in 2.5% glutaraldehyde for electron microscopy. In addition, the remaining intestine was placed in sterile tubes and stored at −80 °C for subsequent enzyme analysis, qPCR, and protein blotting assays.

2.5. Growth performance

Initial body weight (IBW), final body weight (FBW), weight gain rate (WGR), specific growth rate (SGR), feed conversion rate (FCR), survival rate (SR), condition factor (CF), hepatosomatic index (HSI) and visceral index (VSI) were calculated using the formulas (Table 2).

2.6. Hematoxylin and eosin (H&E staining), TUNEL staining, and Oil Red O staining

Initially, the samples were fixed in 4% paraformaldehyde to preserve their integrity. Subsequently, a gradual dehydration process was employed, using a gradient of alcohol to remove excess moisture. To facilitate further processing, the samples were immersed in xylene and then carefully embedded in paraffin wax. Once embedded, the samples were sectioned into 5-μm slices using both room-temperature microtome (Olympus BX43, Tokyo, Japan) and low-temperature microtome (CM1950, Leica Biosystems, Wetzlar, Germany). The sections from the room-temperature microtome were stained with H&E and subjected to terminal deoxynucleotidyl transferase dUTP nick end labeling (TUNEL) to assess cellular characteristics. Simultaneously, sections from the low-temperature microtome were stained with Oil Red O to investigate lipid content. Images were acquired using an automated digital slide scanner (Pannoramic MIDI II, 3D-HISTECH, Hungary) and quantified using ImageJ.

2.7. Immunohistochemical analysis

Immunohistochemical staining for GRP78 (1:100, YT5858, Immunway) was performed using specific antibodies on 4 μm section slides. The detailed program was based on the procedures reported in our previously published article (Zhao et al., 2022b). Sections were scanned using a digital slicing scanner (Pannoramic MIDI II, 3D-HISTECH, Hungary) and imaged. CaseViewer software was used to acquire three images on a 40× field. Image-pro plus 6.0 software (Media Cybernetics Inc, Rockville, MD, USA) was used to analyze the images together with positive immunohistochemical controls.

2.8. Electron microscopy

The samples were immobilized in a solution of 2.5% glutaraldehyde, subjected to dehydration through a gradient of acetone concentrations, and subsequently embedded in resin. Thin sections were then prepared using an ultrathin microtome (UC7rt, LEICA, Germany) and stained with uranyl acetate and lead citrate. The resulting images were captured utilizing an electron transmission microscope (JEM-1400FLASH, JEOL, Japan).

2.9. Serum biochemical indices analysis

Serum glutamate transaminase (GPT), glutamic oxaloacetic transaminase (GOT), alkaline phosphatase (AKP), acid phosphatase

Table 2
Effects on growth performance of largemouth bass (*Micropterus salmoides*).[1]

Items	Groups				
	LC	HC	HCSA	HCSB	HCSASB
IBW, g/fish	7.03 ± 0.036	7.06 ± 0.059	7.02 ± 0.026	7.03 ± 0.013	7.02 ± 0.033
FBW, g/fish	41.00 ± 0.332^{a}	36.17 ± 0.392^{c}	38.09 ± 0.393^{b}	37.86 ± 0.290^{b}	38.35 ± 0.330^{b}
WGR[2], %	483.30 ± 6.137^{a}	412.10 ± 8.389^{c}	442.30 ± 4.079^{b}	438.30 ± 5.133^{bc}	446.10 ± 6.895^{b}
SGR[3], %/day	3.15 ± 0.018^{a}	2.92 ± 0.029^{c}	3.02 ± 0.013^{b}	3.01 ± 0.017^{bc}	3.03 ± 0.023^{b}
FI[4], g/fish	37.13 ± 0.631^{a}	33.92 ± 0.228^{ab}	33.44 ± 0.812^{b}	32.83 ± 0.364^{b}	34.24 ± 1.310^{ab}
FCR[5]	1.09 ± 0.010	1.16 ± 0.012	1.10 ± 0.015	1.11 ± 0.012	1.09 ± 0.033
HSI[6], %	3.11 ± 0.077^{d}	5.49 ± 0.095^{a}	5.24 ± 0.152^{ab}	4.89 ± 0.111^{b}	4.12 ± 0.106^{c}
VSI[7], %	14.32 ± 0.290^{b}	17.31 ± 0.281^{a}	17.20 ± 0.306^{a}	16.59 ± 0.298^{a}	15.41 ± 0.216^{b}
CF[8], g/cm^3	2.32 ± 0.026	2.33 ± 0.015	2.37 ± 0.027	2.33 ± 0.025	2.27 ± 0.020
SR[9], %	97.14 ± 1.732	92.38 ± 1.000	96.19 ± 2.646	97.14 ± 1.732	95.24 ± 2.000

IBW = initial body weight; FBW = final body weight; WGR = weight gain rate; SGR = specific growth rate; FI = feed intake; FCR = feed conversion rate; HSI = hepatosomatic index; VSI = visceral index; CF = condition factor; SR = survival rate.
LC represents a low carbohydrate diet; HC represents a high carbohydrate diet; HCSA, HCSB, and HCSASB represent a high carbohydrate diet supplemented with 2 g/kg SA, 2 g/kg SB, and a combination of 1 g/kg SA and 1 g/kg SB, respectively. SA = sodium acetate; SB = sodium butyrate.
$^{a-d}$Within a row, means without a common superscript differ significantly ($P < 0.05$).
[1] Data were expressed as means ± SEM ($n = 3$ for IBW, FBW, WGR, SGR, FI, FCR, and SR; $n = 9$ for HSI, VSI and CF).
[2] WGR = 100 × (final body weight − initial body weight)/initial body weight.
[3] SGR = 100 × [ln(final weight) − ln(initial weight)]/breeding days.
[4] FI = total amount of dry feed consumed per fish.
[5] FCR = FI/(final body weight − initial body weight).
[6] HSI = liver weight/whole body weight × 100.
[7] VSI = visceral weight/whole body weight × 100.
[8] CF = whole body weight/(body length)^3 × 100.
[9] SR = final number of fish/initial number of fish × 100.

(ACP), and triglycerides (TG) levels were tested following the directions of the manufacturer by using standard kits (Nanjing Jiancheng Bioengineering Institute, China). Immunoglobulin (IgM) and fish complement protein 4 (C4) levels were determined according to the instructions of the enzyme-linked immunoassay (ELISA) kits (Shanghai Enzyme Linked Biotechnology Co., Ltd, China).

2.10. Quantitative real-time PCR

Using our previous genome (unpublished), Primer Premier 5.0 created the primer sequences for qPCR. Details of primers used in this study are shown in Table 3. The Animal Total RNA Isolation Kit (Cat.NO. RE-03014, Foregene, China) was utilized to separate total RNA from intestinal samples, which was then stored for a long period at −80 °C. For qPCR, total RNA was reverse transcribed into cDNA using RT Easy I (Cat.NO. RT-01032, Foregene, China), and kept at −20 °C. The CFX96 real-time PCR detection equipment (BioRad, USA) was then used to carry out real-time quantitative PCR experiments. The target genes were quantified using the ΔCT method, while β-actin was set as a reference gene.

2.11. Western blot

The Western blot procedure was performed according to our previous method (Zhao et al., 2022b). The intestinal tissue was lysed in 500 μL of lysis solution, centrifuged at 12,000 × *g* for 15 min and the supernatants were obtained. Electrophoresis was applied to precast gels. The target protein was transfected onto a PVDF film which was soaked in bovine serum protein for 2 h. The PVDF membrane was then removed, excess primary antibody was washed off with 0.05% Tween20 (TBST), transferred to secondary antibody culture and incubated for 1 h, then washed off again with TBST. Finally, a color developing solution was pipetted to react with the target protein on the PVDF film and images were taken. Data analysis was performed using ImageJ to quantify protein levels. Antibodies: mouse β-actin (1:1,000, 200068-8F10, Zenbio), rabbit bax (1:1,000, #43566, Cell Signaling), rabbit Eif2α (1:500, YT1507, Immunoway), rabbit GRP78 (1:1,000, YT5858, Immunway), rabbit p38-MAPK (1:1,000, Immunoway), rabbit XBP-1 (1:1,000, R1309-10, Huaan Biotechnology), rabbit PPARγ (1:1,000, ET1702-57, Huaan Biotechnology).

2.12. Statistics analysis

The results were expressed as means ± SEM. Shapiro–Wilk test and Levene test were used to check the normal distribution and homogeneity of variance of the data respectively. The *t*-test was utilized to analyze significant differences between the LC and HC groups, and one way ANOVA was utilized to examine significant differences amongst the HC, HCSA, HCSB, and HCSASB groups. Data were compared using Duncan multiple range test, with "*" denoting statistical differences among the LC and HC groups (*$P < 0.05$, **$P < 0.01$). Means without a common superscript differ significantly ($P < 0.05$). All data were statistically analyzed by GraphPad Prism 9.1.

3. Results

3.1. Growth performance

After 8 weeks of feeding, FCR, CF, and SR (Table 2) did not differ significantly among the groups ($P > 0.05$). The results of the growth performance analysis (Table 2) indicated that FBW, WG, and specific growth rate (SGR) were significantly lower in the HC group than in the low-carbohydrate diet (LC) group ($P < 0.05$). However, FBW was significantly higher in the HC diet supplemented with 2 g/kg sodium acetate (HCSA), 2 g/kg sodium butyrate (HCSB), and a combination of 1 g/kg sodium acetate and 1 g/kg sodium butyrate (HCSASB) groups ($P < 0.05$) than in the HC group, whereas WGR and SGR were significantly higher in the HCSA and HCSASB groups than in the HC group ($P < 0.05$).

VSI and HSI were significantly higher in the HC group than in the LC group ($P < 0.05$), and HSI was significantly lower in both the HCSB and HCSASB groups ($P < 0.05$), although VSI was significantly lower in the HCSASB group than in the HC group ($P < 0.05$).

3.2. Serum parameters

The serum AKP, ACP, GOT, and GPT levels were significantly higher in the HC group than in the LC group ($P < 0.05$); after treatment, AKP and GPT were significantly lower in the HCSA, HCSB, and HCSASB groups ($P < 0.05$). ACP was significantly lower in the HCSB group ($P < 0.05$), and GOT was significantly lower in the HCSASB group ($P < 0.05$, Fig. 1A to D). IgM and C4 were higher in the HC group and the three treatment groups than in the LC group, but only C4 was markedly higher in the HCSB and HCSASB groups than in the HC group ($P < 0.05$, Fig. 1E and F).

3.3. Gut morphology and physical barrier

Pathological changes in the gut were analyzed. Intestinal villus height as shown by HE staining was markedly reduced in the HC group compared with the LC group ($P < 0.05$), while this was restored by treatment with SA, SB, and SASB (Fig. 2A and C). The widths of the intestinal villi were not markedly different ($P > 0.05$) among the experimental groups (Fig. 2A and C). The intestinal microvilli in the HC group were also shown by transmission electron microscopy to be disorganized and partially detached, exhibiting an irregular state, while in the other four groups, these were relatively cleanly arranged and uniform in length (Fig. 2B). Meanwhile, the lengths of intestinal microvilli in the HC group were less than those in the LC group ($P > 0.05$, Fig. 2B and D), while the intestinal microvilli in the HCSA, HCSB, and HCSASB groups were greater in length than those in the HC group, although the differences were not significant ($P > 0.05$, Fig. 2B and D). We also examined tight junction (TJ)-related genes to assess intestinal barrier integrity. We found that the gene expression levels of zonula occludens-1 (*ZO-1*), occludin, and claudin-7 were significantly lower in the group fed HC than in the LC group ($P < 0.05$, Fig. 2E), but the levels were notably higher in the HCSB and HCSASB groups than in the HC group ($P < 0.05$, Fig. 2E).

3.4. Intestinal endoplasmic reticulum stress

There was a noticeable increase in the mRNA expression levels of ERS-related genes (*ATF6*, *XBP-1*, *GRP78*, *CHOPα*, and *Eif2α*) in the HC group compared with the LC group ($P < 0.05$, Fig. 3A). After SA and SB treatment, the mRNA expression levels of *XBP-1*, *GRP78*, and *CHOPα* in the HCSA, HCSB, and HCSASB groups were significantly decreased ($P < 0.05$, Fig. 3A), whereas the expression levels of *ATF6* and *Eif2α* mRNA were significantly downregulated in the HCSASB group ($P < 0.05$, Fig. 3A). We then examined the ERS marker GRP78. Using immunohistochemical analysis, positive GRP78 expression was found to be significantly higher in the HC group than in the LC group ($P < 0.05$, Fig. 3B), while the positive expression was lower in the HCSA, HCSB, and HCSASB groups than in the HC group ($P < 0.05$, Fig. 3B). It is important to note that XBP-1 and Eif2α, key regulators of the ERS response, had protein expression levels that were remarkably increased in the HC group but decreased in the HCSA, HCSB, and HCSASB groups ($P < 0.05$, Fig. 3C to E).

Table 3
Primer sequences used for real-time PCR analysis.

Gene	Primer sequence (5′ to 3′)	Tm, °C	Amplicon size, bp	E-value, %	R^2	GenBank no.
β-Actin	F: AAAGGGAAATCGTGCGTGAC R: AAGGAAGGCTGGAAGAGGG	61	102	99.8	0.995	XM_020154709.1
ZO-1	F: ATCTCAGCAGGGATTCGACGGCTG R: CTTTTGCGCTGGCGTTGG	58.0	149	98.0	0.982	XM_038701018.1
Occludin	F: ACTTTGGATTACCTGCG R: GGGAGGGGCAAGACAACAGT	60.3	154	99.2	0.996	XM_038734217.1
Claudin-*7*	F: CATTTCAGCAAACACATC R: CGGCACAGAAATCCCAGAG	58.4	92	99.2	0.995	XM_038715821.1
ATF6	F: CAGGACGAAGTGCTTAGAGTT R: AGAGTAATGGACGGTCACAAT	64.3	145	97.9	0.985	XM_038716053.1
IRE1	F: ACGGACCAATCGTGAGAC R: CGGGAGGTGAAGTAGGAG	60.6	168	100.2	0.987	XM_038712961.1
XBP-1	F: ACACCCTCGACACGAAAGA R: AGAATGCCCAGTAGCAAATC	57.7	106	99.8	0.996	XM_038703562.1
GRP78	F: TTGCCGATGACGACGAAA R: CAATCAGACGCTCACCCT	60.6	82	99.4	0.995	NW_024041151.1
CHOPα	F: GATGAGCAGCCTAAGCCACG R: AACAGGTCAGCCAAGAAGTCG	63.0	165	100.1	0.998	XM_038697521.1
Eif2α	F: CCTCGTTTGTCCGTCTGTATC R: GCTGACTCTGTCGGCCTTG	57.7	85	99.8	0.991	PRJNA725023
bax	F: ACTTTGGATTACCTGCGGGA R: TGCCAGAAATCAGGAGCAGA	61.0	106	100.5	0.989	XM_038704178.1
bcl2	F: CGCCATCCACAGAGTCCT R: CCGGAACAGTTCGTCTATCACC	59.4	145	97.8	0.995	XM_038695757.1
caspase3	F: GCTTCATTCGTCTGTGTTC R: CGAAAAAGTGATGTGAGGTA	54.0	187	98.4	0.992	XM_038713063.1
caspase8	F: GAGACAGACAGCAGACAACCA R: TTCCATTTCAGCAAACACATC	56.0	156	98.8	0.996	XM_038718636.1
caspase9	F: CTGGAATGCCTTCAGGAGACGGG R: GGGAGGGGCAAGACAACAGGGTG	66.0	178	99.5	0.987	XM_038723308.1
NF-κB	F: TGATGATAACTGGCTTCGG R: TCAAACCTGGACCCTACCT	60.6	178	100.6	0.998	XM_038723088.1
p38-MAPK	F: CCCCACAACAAGAATCATGC R: TCTCAGCCTTCTCGTGGA	58	180	100.1	0.989	XM_038728055.1
Hepcidin1	F: CATTCACCGGGGTGCAA R: CCTGATGTGATTTGGCATCATC	58.0	140	98.9	0.991	XM_038710826.1
COX2	F: CACTGGGTCGTGTCACTTT R: TGATTCTCCTCCTTGCTGT	60.6	140	99.5	0.995	YP_636060.1
CD80	F: TCTTCATCGTGGTAATAATAGG R: TGTGGTGTCTTCAGGGTCT	58.0	142	99.6	0.989	EVM_0001828.1
IL-8	F: CGTTGAACAGACTGGGAGAGATG R: AGTGGGATGGCTTCATTATCTTGT	64.0	123	100.1	0.982	XM_038704089.1
FAS	F: TGATGATAACTGGCTTCGG R: TCAAACCTGGACCCTACCT	60.6	86	100.1	0.995	XM_038735140.1
ACCA	F: CACCAGGAACATATCGGACA R: ATCAATGTCGCTGTCAGTCT	63.0	184	99.7	0.994	XM_038709737.1
SCD1	F: CGCCGAAGATGATGGTGT R: GGAAGACTCGCAGTGGATTAG	63.0	153	98.9	0.998	XM_038735580.1
PPARγ	F: AGCAGACATCCGCCCTAA R: ACCTCGATCACGCCGTAC	64.3	160	100.4	0.997	XM_038695878.1
CPT1α	F: AGCCCCACCCCAACCTACCAG R: CGGCCCTCACGGAATAAACGC	65.0	81	98.2	0.991	XM_038695351.1
HSL	F: TACCCTCCGTGGCCTTTGACC R: CTCGTCTTCAGCCCCAGCGAT	64.0	161	99.5	0.987	XM_038725628.1
AMPKα	F: CACATGAATGCCAAGATTG R: GGACCAGCATATAACCTTC	54.7	165	99.6	0.995	XM_038734014.1
PGC1α	F: AGATTCAGGGCTAGATATGGG R: GGAAGAGTGGGCTTGGTG	63.0	189	98.9	0.997	XM_038731662.1
PPARα	F: CCACCGCAATGGTCGATATG R: TGCTGTTGATGGACTGGGAAA	58.0	156	100.2	0.993	XM_038738333.1

F = forward primer; R = reverse primer; Tm = melting temperature; *ZO-1* = zonula occludens-1; *ATF6* = activating transcription factor 6; *IRE1* = inositol-requiring enzyme 1; *XBP-1* = x-box binding protein 1; *GRP78* = glucose related protein 78; *CHOPα* = C/EBP homologous protein alpha; *Eif2α* = eukaryotic initiation factor 2 alpha; *bax* = bcl2-associated x protein; *bcl2* = b-cell lymphoma-2; *caspase3* = cysteine aspastic acid-specific protease 3; *caspase8* = cysteine aspastic acid-specific protease 8; *caspase9* = cysteine aspastic acid-specific protease 9; *NF-κB* = nuclear factor kappa-B; *p38-MAPK* = mitogen-activated protein kinases; *COX2* = cyclooxygenase 2; *CD80* = CD80 molecule; *IL-8* = interleukin 8; *FAS* = fatty acid synthase; *ACCA* = acetyl-CoA carboxylase; *SCD1* = stearoyl-CoA desaturase-1; *PPARγ* = peroxisome proliferator-activated receptor γ; *CPT1α* = carnitine palmitoyl transferase-1 alpha; *HSL* = hormone-sensitive lipase; *AMPKα* = adenosine 5-monophosphate (AMP)-activated protein kinase alpha; *PGC1α* = peroxisome proliferators-activated receptor γ coactivator 1 alpha; *PPARα* = peroxisome proliferator-activated receptor-alpha.

3.5. Intestinal electron microscopy

The changes in intestinal structure and organelles were further observed using a transmission electron microscope. The results showed that the borders between intestinal epithelial cells in the LC group were clear, and tightly interconnected structures were visible; the mitochondria were oval; and the cristae were intact. Furthermore, the matrix electron density was moderate; the double-layered membrane structure was intact; the number of lysosomes was high; and the rough endoplasmic reticulum did not

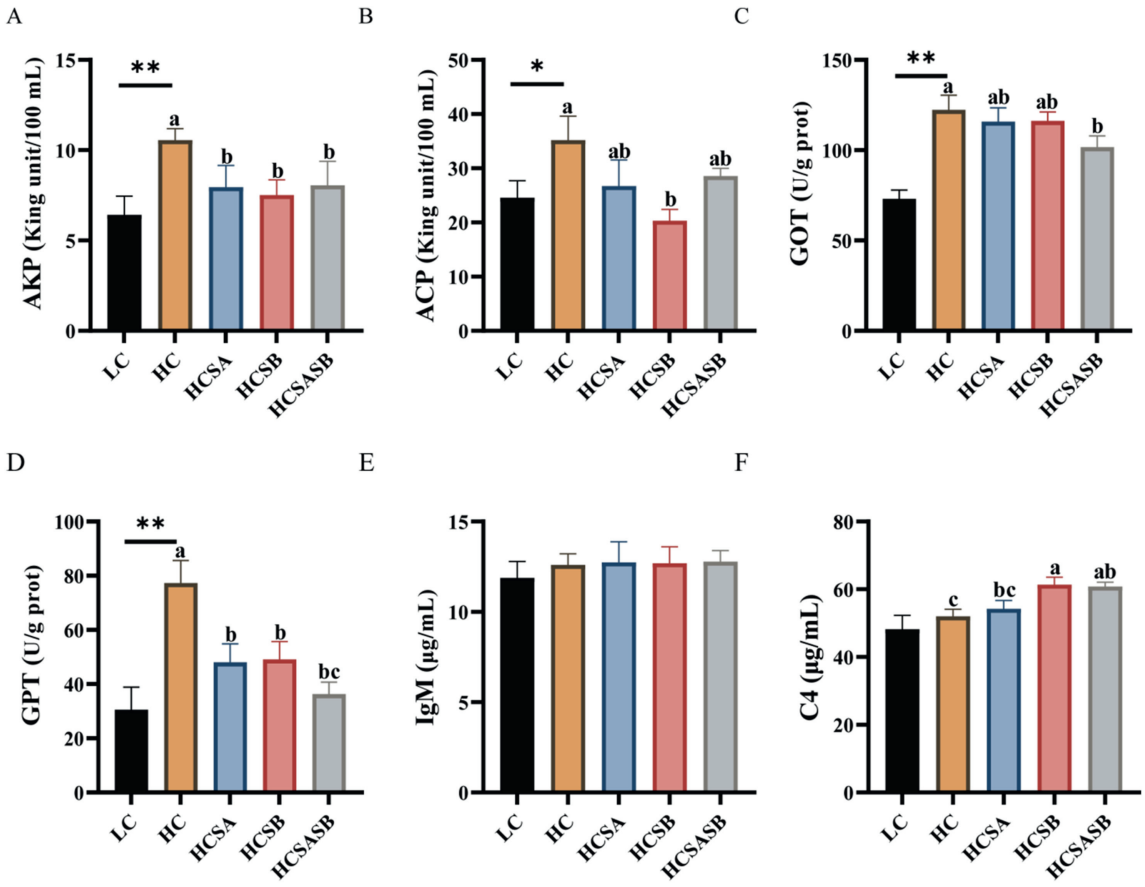

Fig. 1. Effect of dietary sodium acetate (SA) and sodium butyrate (SB) on serum biochemical parameters of largemouth bass fed a high carbohydrate diet. LC represents a low carbohydrate diet; HC represents a high carbohydrate diet; HCSA, HCSB, and HCSASB represent a high carbohydrate diet supplemented with 2 g/kg SA, 2 g/kg SB, and a combination of 1 g/kg SA and 1 g/kg SB, respectively. (A) Alkaline phosphatase (AKP). (B) Acid phosphatase (ACP). (C) Glutamic oxaloacetic transaminase (GOT). (D) Glutamate transaminase (GPT). (E) Immunoglobulin (IgM). (F) Fish complement protein 4 (C4). Data were expressed as means ± SEM ($n = 6$). Asterisk indicates statistical differences between LC and HC groups (*$P < 0.05$, **$P < 0.01$). $^{a-c}$Means without a common superscript differ significantly ($P < 0.05$).

show pronounced swelling (Fig. 4). In contrast, the borders between intestinal epithelial cells in the HC group were blurred; most of the mitochondria were swollen; the cristae were ruptured or disappeared, showing vacuolization; and the number of lysosomes was notably lower than that in the LC group (Fig. 4). In contrast to the HC group, the HCSA, HCSB, and HCSASB groups showed some improvement but less than that of the LC group.

3.6. Intestinal apoptosis and inflammation

The results of the TUNEL assay indicated that the level of intestinal apoptosis was significantly higher in the HC group than in the LC group ($P < 0.05$), whereas the SA, SB, and SASB diets significantly inhibited apoptosis induced by HC ($P < 0.05$, Fig. 5A and B). Therefore, we investigated the expression levels of the most important genes and proteins involved in apoptosis. There was a significant upregulation of the mRNA expression levels of *bcl2*, *bax*, *caspase3*, *caspase8*, and *caspase9* in the HC group compared with the LC group ($P < 0.05$). After SA and SB treatment, the mRNA expression levels of *bax*, *caspase3*, and *caspase9* in the HCSA, HCSB, and HCSASB groups were significantly decreased compared with those in the HC group ($P < 0.05$), while the mRNA expression levels of *bcl2* and *caspase8* in the HCSASB group were significantly decreased compared with those in the HC group ($P < 0.05$, Fig. 5C). Likewise, the levels of key pro-apoptotic bax proteins were remarkably upregulated in the HC group ($P < 0.05$), while dietary SA, SB, and SASB significantly inhibited their expression ($P < 0.05$, Fig. 5E and F).

The mRNA expression levels of *NF-κB* and *p38-MAPK* were significantly higher in the HC group than in the LC group ($P < 0.05$). However, after three treatments, the mRNA and protein expression levels of p38-MAPK were significantly lower in the HCSA, HCSB, and HCSASB groups than in the HC group ($P < 0.05$, Fig. 5D, E, G), whereas only the expression levels of *NF-κB* mRNA were lower in the HCSB group than in the HC group ($P < 0.05$, Fig. 5D). There was a significant upregulation of the mRNA expression levels of pro-inflammatory genes (Hepcidin1, *COX2*, *CD80*, and *IL-8*) in the HC group ($P < 0.05$). However, after all three treatments, their expression levels were significantly lower than in the HC group ($P < 0.05$, Fig. 5D).

3.7. Intestinal lipid metabolism

There was a marked increase in intestinal fat content in the HC group as demonstrated by Oil Red O staining ($P < 0.05$), whereas the HCSA, HCSB, and HCSASB groups had lower intestinal fat contents than the HC group, and the contents were significantly less in the HCSB and HCSASB groups than in the HC group ($P < 0.05$, Fig. 6A and B). A similar pattern was observed for intestinal TG content (Fig. 6C). Furthermore, genes related to lipogenesis (*FAS*, *ACCA*, *SCD1*, and *PPARγ*) were significantly upregulated in the HC group compared with the LC group ($P < 0.05$), but SA and SB significantly

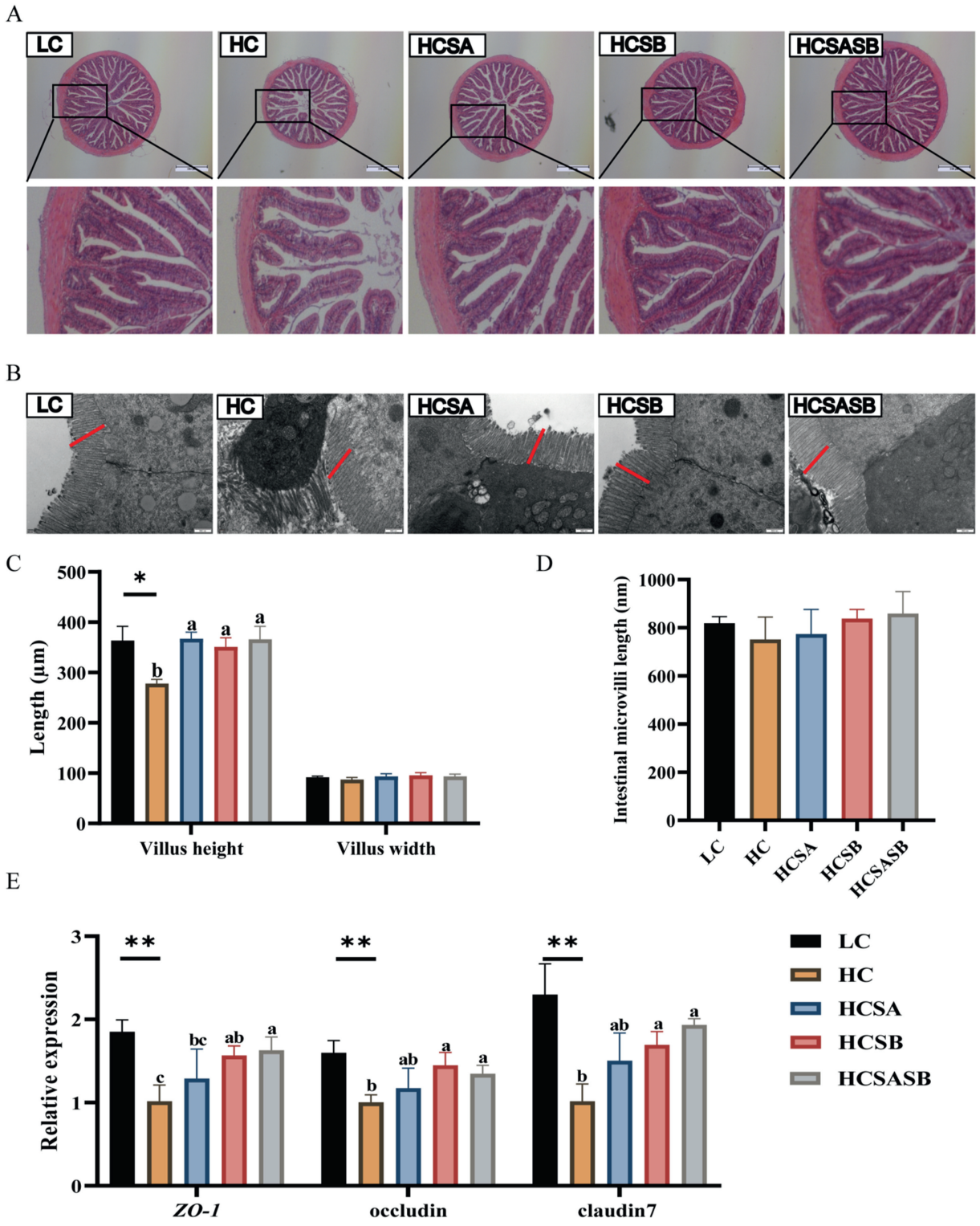

Fig. 2. Dietary sodium acetate (SA) and sodium butyrate (SB) improved intestinal morphology and attenuated barrier damage in largemouth bass fed a high carbohydrate diet. LC represents a low carbohydrate diet; HC represents a high carbohydrate diet; HCSA, HCSB, and HCSASB represent a high carbohydrate diet supplemented with 2 g/kg SA, 2 g/kg SB, and a combination of 1 g/kg SA and 1 g/kg SB, respectively. (A) H&E staining images of intestinal sections (scale bars, 500 μm). (B) Transmission electron microscopy images of intestinal microvilli (scale bars, 500 nm). (C) Intestinal villi height and width. (D) Height of intestinal microvilli. (E) Expression levels of tight junction-related genes. Data were expressed as means ± SEM ($n = 6$). Asterisk indicates statistical differences between LC and HC groups (*$P < 0.05$, **$P < 0.01$). $^{a-c}$Means without a common superscript differ significantly ($P < 0.05$). *ZO-1* = zonula occludens-1.

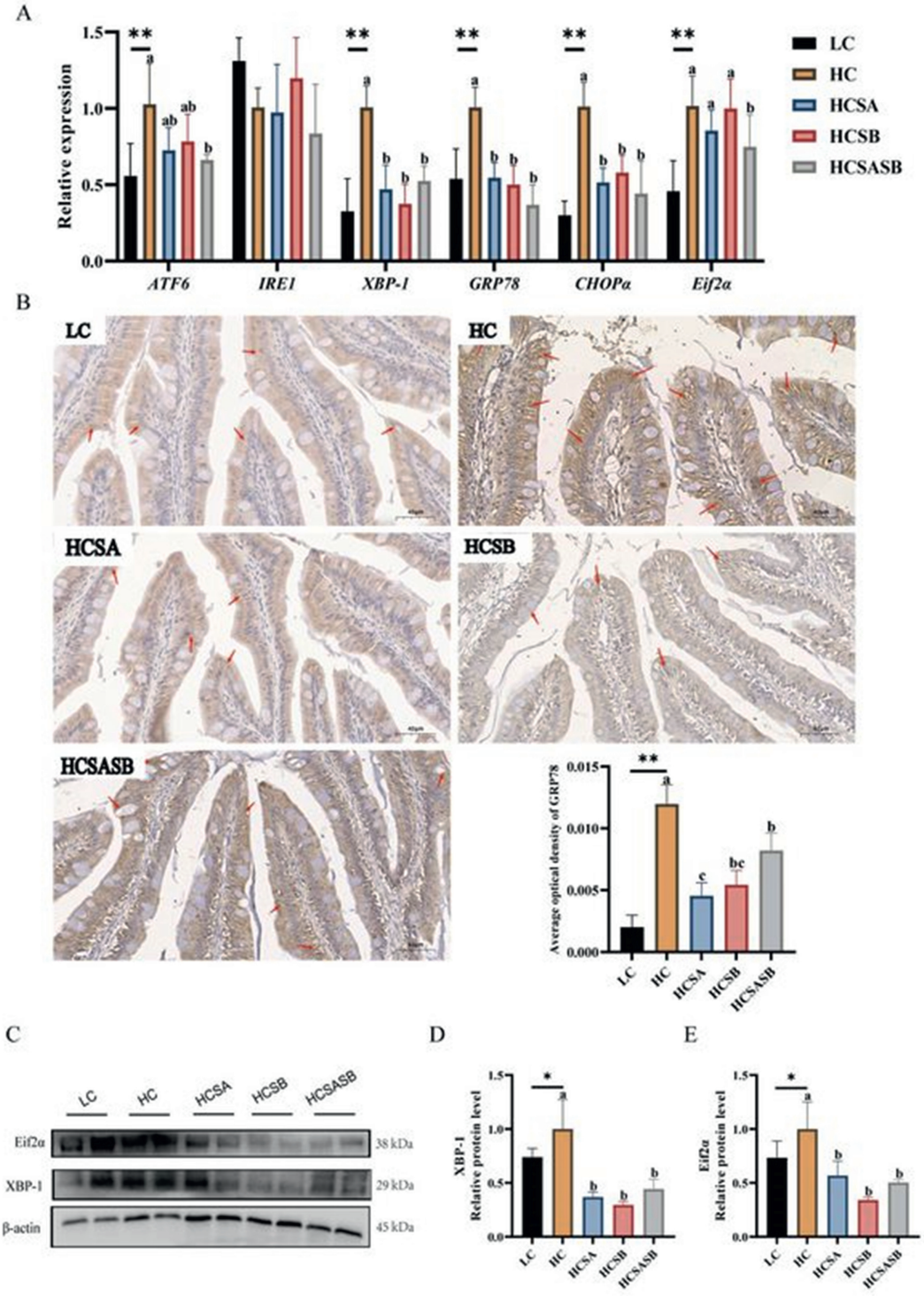

Fig. 3. Dietary sodium acetate (SA) and sodium butyrate (SB) alleviated high carbohydrate (HC)-induced intestinal endoplasmic reticulum stress in largemouth bass. LC represents a low carbohydrate diet; HC represents a high carbohydrate diet; HCSA, HCSB, and HCSASB represent a high carbohydrate diet supplemented with 2 g/kg SA, 2 g/kg SB, and a combination of 1 g/kg SA and 1 g/kg SB, respectively. (A) Expression levels of intestinal endoplasmic reticulum stress related genes. (B) Intestinal GRP78 immunohistochemistry (the tail of the arrow represent positive expression. Scale bars, 20 μm). (C-E) Expression levels of XBP-1 and Eif2α protein. Data were expressed as means ± SEM ($n = 6$). Asterisk indicates statistical differences between LC and HC groups (*$P < 0.05$, **$P < 0.01$). $^{a-c}$Means without a common superscript differ significantly ($P < 0.05$). *ATF6* = activating transcription factor 6; *IRE1* = inositol-requiring enzyme 1; *XBP-1* = x-box binding protein 1; *GRP78* = glucose related protein 78; *CHOPα* = C/EBP homologous protein alpha; *Eif2α* = eukaryotic initiation factor 2 alpha.

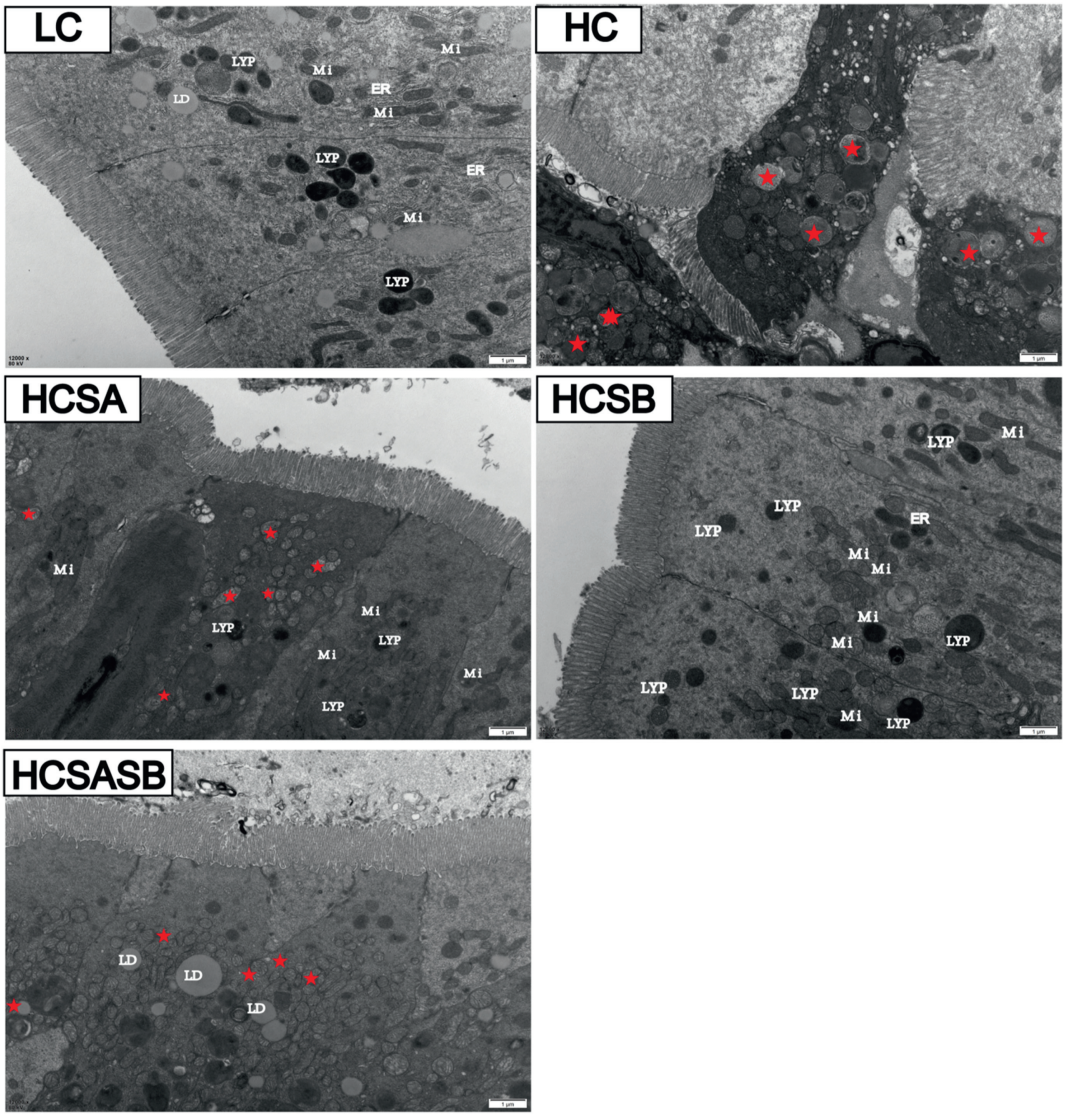

Fig. 4. Electron micrographs of largemouth bass guts (scale bars, 1 μm). The red pentagons represent mitochondrial damage. LC represents a low carbohydrate diet; HC represents a high carbohydrate diet; HCSA, HCSB, and HCSASB represent a high carbohydrate diet supplemented with 2 g/kg SA, 2 g/kg SB, and a combination of 1 g/kg SA and 1 g/kg SB, respectively. SA = sodium acetate; SB = sodium butyrate; Mi = mitochondria; ER = endoplasmic reticulum; LYP = lysosome; LD = lipid droplet.

reduced the expression of lipogenesis genes ($P < 0.05$, Fig. 6D). In addition, lipolysis-related genes showed an opposite trend to lipogenesis-related genes, with the expression levels of lipolysis-related genes (*CPT1α*, *HSL*, *AMPKα*, and *PPARα*) significantly lower in the HC group than in the LC group ($P < 0.05$) but significantly greater in the HCSA, HCSB, and HCSASB groups ($P < 0.05$, Fig. 6E). It is important to note that the protein level of the key adipogenic factor PPARγ was also significantly upregulated in the HC group ($P < 0.05$), while its expression was significantly inhibited by dietary SA and SB ($P < 0.05$, Fig. 6F and G).

4. Discussion

The addition of moderate amounts of carbohydrates to aquatic feeds not only saves protein dosage but also reduces ammonia nitrogen emissions from aquatic animals that in turn reduces the pollution from farmed water bodies (Ali and Jauncey, 2004). However, a chronic HC diet can cause metabolic abnormalities in fish and impair immune function, thereby affecting gut health and eventually causing a reduction in growth rate (Wang et al., 2021; Xie et al., 2017). SA and SB can be rapidly absorbed by the intestinal tract of aquatic animals, and play important roles in regulating host metabolism, immune response and improving intestinal function (Xun et al., 2023; Zhang et al., 2020; Zhao et al., 2021a; Zhou et al., 2023). Therefore, we assessed the efficacy of adding SA and SB to a HC diet on the intestinal health of juvenile largemouth bass. Our study demonstrated that dietary SA and SB ameliorated HC-induced intestinal inflammation, apoptosis, and lipid metabolism disorders by reducing intestinal ERS. Although both SA and SB can alleviate the intestinal damage caused by HC, there is no significant difference between the two.

4.1. SA and SB enhanced the growth performance of HC-fed juvenile largemouth bass

SA and SB have been extensively studied in the aquaculture industry due to their effectiveness and safety. Many studies have shown that SA is catabolic in other tissues and organs after

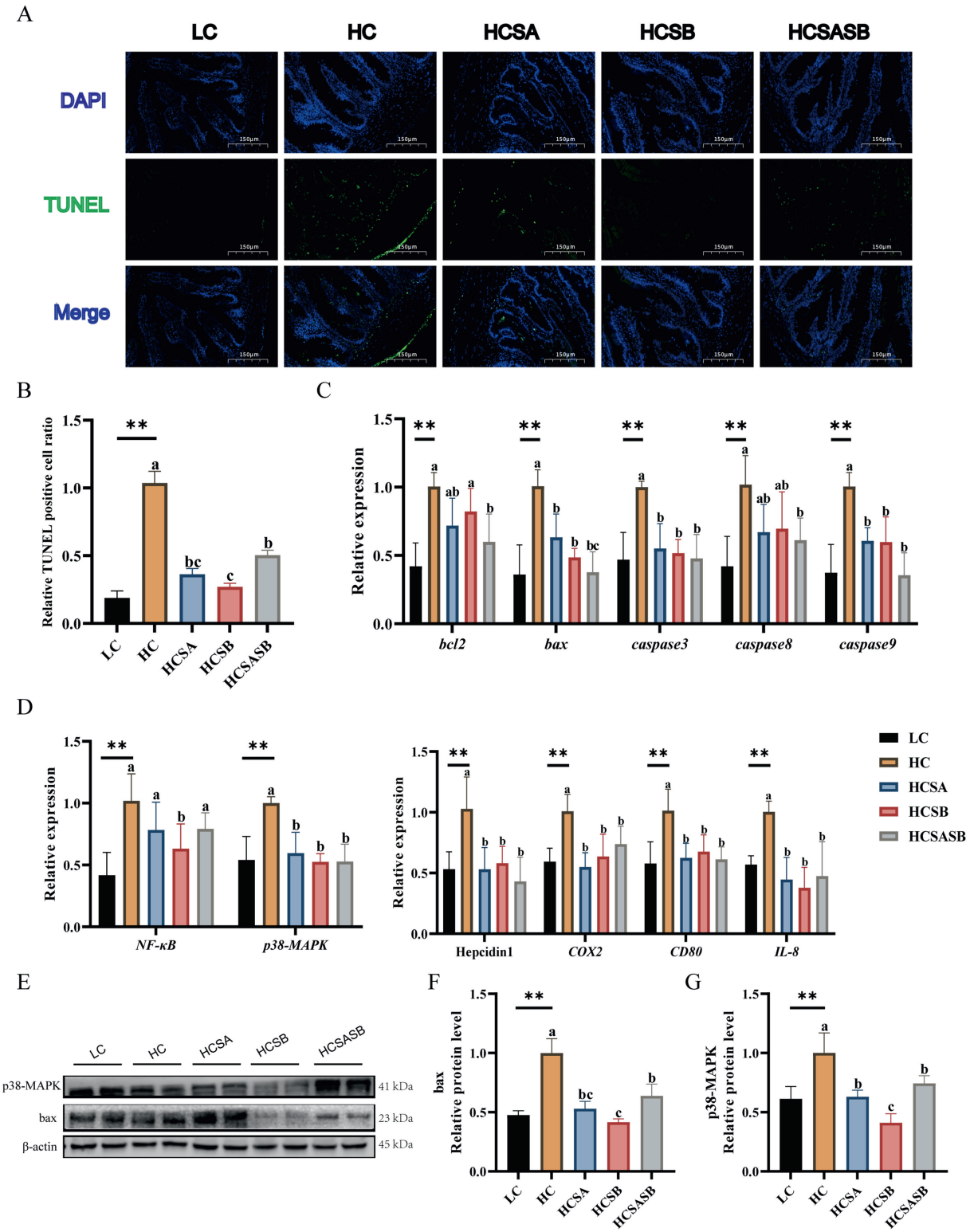

Fig. 5. Dietary sodium acetate (SA) and sodium butyrate (SB) ameliorated high carbohydrate-induced apoptosis and inflammation in largemouth bass. LC represents a low carbohydrate diet; HC represents a high carbohydrate diet; HCSA, HCSB, and HCSASB represent a high carbohydrate diet supplemented with 2 g/kg SA, 2 g/kg SB, and a combination of 1 g/kg SA and 1 g/kg SB, respectively. (A) TUNEL (green) stained images of intestinal sections (scale bars, 50 μm). (B) Relative apoptosis rates in intestinal sections. (C) Expression levels of intestinal apoptosis related genes. (D) Expression levels of intestinal NF-κB and p38-MAPK genes and pro-inflammatory related genes. (E to G) Expression levels of intestinal bax and p38-MAPK proteins. Data were expressed as means ± SEM ($n = 6$). Asterisk indicates statistical differences between LC and HC groups (*$P < 0.05$, **$P < 0.01$). $^{a-c}$Means without a common superscript differ significantly ($P < 0.05$). *bax* = bcl2-associated x protein; *bcl2* = b-cell lymphoma-2; *caspase3* = cysteine aspastic acid-specific protease 3; *caspase8* = cysteine aspastic acid-specific protease 8; *caspase9* = cysteine aspastic acid-specific protease 9; *NF-κB* = nuclear factor kappa-B; *p38-MAPK* = mitogen-activated protein kinases; *COX2* = cyclooxygenase 2; *CD80* = CD80 molecule; *IL-8* = interleukin 8.

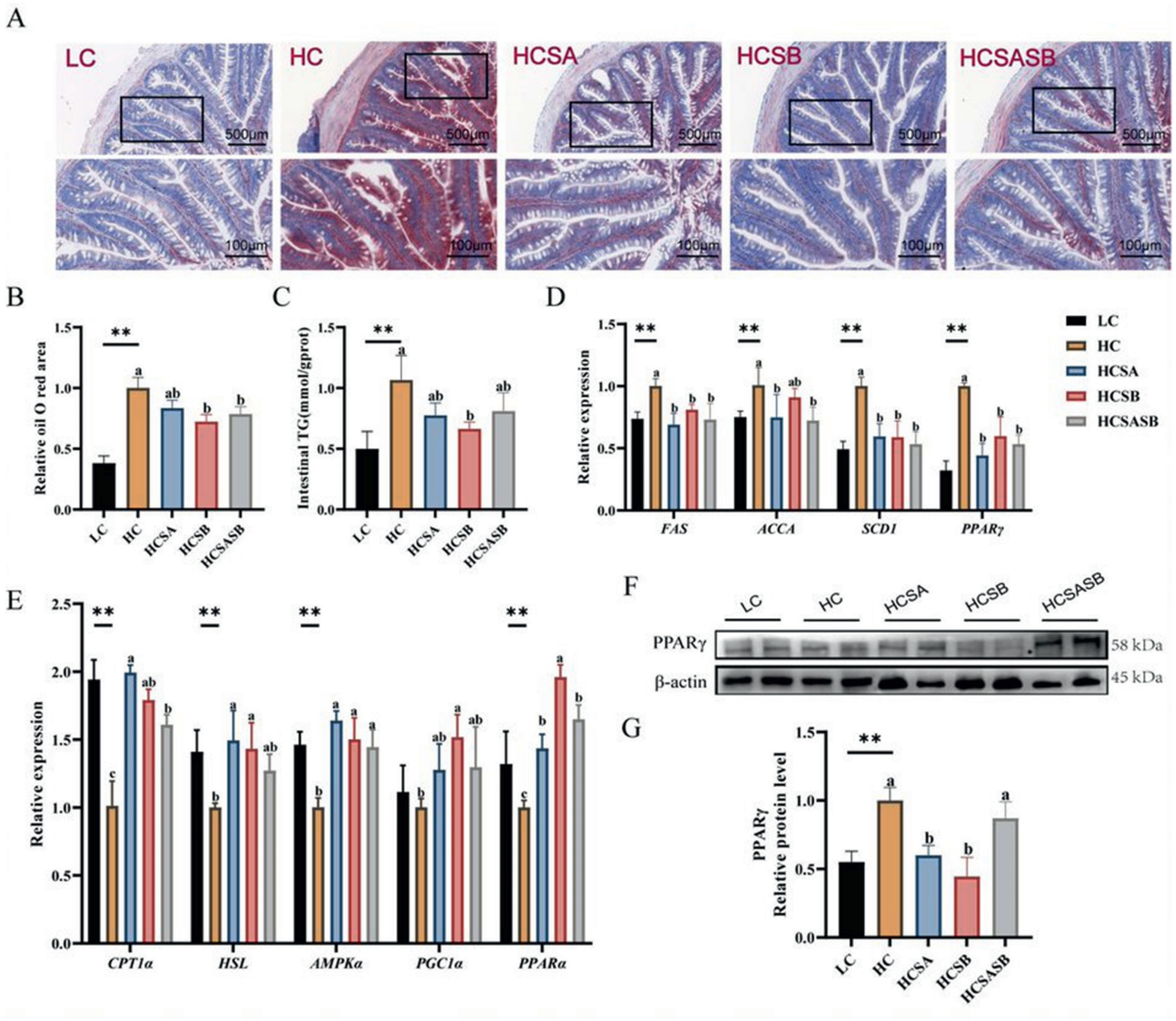

Fig. 6. Dietary sodium acetate (SA) and sodium butyrate (SB) ameliorated high carbohydrate-induced intestinal lipid deposition in largemouth bass. LC represents a low carbohydrate diet; HC represents a high carbohydrate diet; HCSA, HCSB, and HCSASB represent a high carbohydrate diet supplemented with 2 g/kg SA, 2 g/kg SB, and a combination of 1 g/kg SA and 1 g/kg SB, respectively. (A) Oil-red O staining images of intestinal sections (scale bars, 500 μm). (B) Relative oil-red O area in intestinal sections. (C) Intestinal triglycerides (TG) levels. (D) Expression levels of adipogenic related genes. (E) Expression levels of lipolytic related genes. (F, G) Expression level of PPARγ protein. Data were expressed as means ± SEM ($n = 6$). Asterisk indicates statistical differences between low carbohydrate (LC) and high carbohydrate (HC) groups (*$P < 0.05$, **$P < 0.01$). $^{a-c}$Means without a common superscript differ significantly ($P < 0.05$). *FAS* = fatty acid synthase; *ACCA* = acetyl-CoA carboxylase; *SCD1* = stearoyl-CoA desaturase-1; *PPARγ* = peroxisome proliferator-activated receptor γ; *CPT1α* = carnitine palmitoyl transferase-1 alpha; *HSL* = hormone-sensitive lipase; *AMPKα* = adenosine 5-monophosphate (AMP)-activated protein kinase alpha; *PGC1α* = peroxisome proliferators-activated receptor γ coactivator l alpha; *PPARα* = peroxisome proliferator-activated receptor alpha.

absorption in the blood, and is an important energy source for the host (Park et al., 2015). However, SB is the main source of energy metabolism in intestinal epithelial cells. In addition, SA and SB can also improve the enzyme activity of intestinal digestive enzymes, promote nutrient absorption, and improve growth performance (Estensoro et al., 2016; Feng et al., 2022a; Robles et al., 2013). The present research revealed that the HC group of largemouth bass demonstrated substantially reduced growth parameters (FBW, WG, and SGR) compared with the LC group, in agreement with previous studies (Feng et al., 2022b; Liang et al., 2022). However, supplementation with SA and SB significantly improved growth performance, as has been observed in studies with zebrafish, Nile tilapia, and yellow catfish (Abdel-Tawwab et al., 2021; Zhang et al., 2020; Zhao et al., 2021b). Interestingly, SA and SB were equally effective in the growth promotion of juvenile largemouth bass. In addition, dietary SA and SB reversed the abnormally high body indices (HSI and VSI) caused by HC. Similarly, SB reduced HSI and VSI in largemouth bass fed a high-fat diet (Chen et al., 2023).

4.2. SA and SB alleviated immune disorders caused by HC

The analysis of serum parameters helps to assess the overall health status of the animal. Alkaline phosphatase and ACP are two important immunomodulatory enzymes that help eliminate pathogens during the immune response (Fu et al., 2017). Glutamate transaminase and GOT are two major metabolic enzymes that are frequently used to assess the organismal health of fish (Zhao et al., 2021d). Metabolic and immune disorders may lead to abnormally elevated activities of these enzymes (Lin et al., 2018). The present research found that intake of HC resulted in abnormally elevated

serum AKP, ACP, GPT, and GOT levels, but treatment with SA and SB restored these to relatively normal states. Similarly, studies on yellow catfish and grass carp also revealed that the dietary supplementation of SA and SB reduced the abnormal elevation of these enzymes caused by external stress (Tian et al., 2017; Zhao et al., 2021a). In addition, the immune system, particularly the humoral adaptive immune system, is largely composed of C4 and IgM (Boshra et al., 2006; Zhou et al., 2013). In this study, we found no significant changes in C4 or IgM in the HC group compared with the LC group, but the addition of SA and SB to the diet resulted in enhanced IgM activity and significantly higher C4 activity. Conversely, it has been shown that dietary carbohydrate was negatively correlated with serum IgM and C4 activity (Zhou et al., 2013), possibly due to the variation in tolerance to carbohydrate levels in different fish species. However, studies on crucian carp and European seabass showed that serum innate immune parameters, including IgM and C4, were elevated to some extent after the addition of short-chain fatty acids to the diets, consistent with our results (Abdel-Mohsen et al., 2018; Li et al., 2022b). Thus, these findings suggest that dietary SA and SB can alleviate HC-induced immune disorders to the same extent and enhance non-specific immunity in largemouth bass.

4.3. SA and SB attenuated HC-induced intestinal barrier damage

Gut health is known to be closely linked to performance, feed efficiency, and general health, and excessive carbohydrate intake can affect fish gut metabolism and physiology (Zhang et al., 2023; Zhao et al., 2020b). Previous studies have demonstrated that HC can damage intestinal villi and microvilli in yellow catfish and largemouth bass (Zhou et al., 2021). Similarly, in this study, HC reduced intestinal villus height and microvillus length, but all of these effects were reversed by dietary SA and SB. Studies have shown that SA and SB are converted into ketone bodies (acetoacetic acid, β-hydroxybutyric acid) in the liver, which serve as the main fuel source of intestinal oxidative metabolism, providing energy for intestinal growth and promoting intestinal development (Zhang et al., 2019). These results suggest that SA and SB can protect against HC-induced atrophy of intestinal villi and microvilli. In addition, the oversupply of carbohydrates as an energy source can lead to chronic stress, resulting in damage to the intestinal barrier that is largely governed by the TJ protein that connects epithelial cells (Oshima et al., 2008; Suzuki, 2013). Further studies showed that SA and SB reduced HC-induced TJ reduction by increasing the expression levels of *ZO-1*, occludin, and claudin-7 genes. Interestingly, similar findings were obtained from studies on broilers (Zou et al., 2019), grass carp (Wu et al., 2018), and mice (Chen et al., 2022), where SA and SB markedly increased the expression of TJ-related genes in the intestine. Thus, our results suggest that dietary SA and SB improved HC-induced intestinal morphology and intestinal barrier function in largemouth bass.

4.4. SA and SB ameliorated HC-induced intestinal ERS, apoptosis, and inflammation and improved lipid metabolism

Previous reports have demonstrated that a chronic HC diet induces intestinal ERS in fish such as largemouth bass, large yellow croaker, and yellow catfish (Zhao et al., 2021c; Fang et al., 2021; Zhao et al., 2020b). In addition, similar studies have been reported in mammals, and ERS has been shown to be strongly correlated with intestinal injury (Huang et al., 2019; Song et al., 2022). Therefore, we hypothesized that HC-induced intestinal injury, including intestinal inflammation, apoptosis, and disorders of lipid metabolism, is attributed to excessive activation of ERS. Hence, we investigated the ERS status to further explore the potential mechanisms of SA and SB in attenuating HC-induced intestinal injury. In this study, ERS-related genes (*ATF6*, *XBP-1*, *GRP78*, *CHOPα*, and *Eif2α*) and key proteins (XBP-1, GRP78, and Eif2α) were markedly upregulated in the HC group, but intestinal ERS was significantly alleviated in juvenile largemouth bass following the addition of SA and SB to the diet. Previous studies have demonstrated that SA and SB can ameliorate tissue damage by attenuating ERS in the brain, liver, and intestine of mice (Hu et al., 2018; Wu et al., 2021; Zhang et al., 2016). However, few studies have examined the effect of adding SA and SB to the diet on ameliorating HC-induced intestinal ERS in fish. Our results suggest that SA and SB can alleviate intestinal HC-induced ERS in largemouth bass, thereby providing an empirical basis for ameliorating intestinal damage.

Chronic inflammation, apoptosis, and excessive lipid deposition are closely associated with ERS (Jia et al., 2020; Medzhitov, 2008; Sano and Reed, 2013). In aquaculture species, a HC diet induced intestinal and hepatic inflammation and apoptosis in eels, Nile tilapia, and largemouth bass (Lin et al., 2018; Shi et al., 2022b; Wang et al., 2022). In the present study, the HC group displayed upregulated expression of pro-inflammatory genes (hepcidin1, *COX2*, *CD80*, and *IL-8*) through NF-κB and p-38MAPK signaling pathways, while dietary SA and SB inhibited the expression of pro-inflammatory factors in the intestine of largemouth bass, significantly ameliorating HC-induced intestinal inflammation. Similarly, studies on Nile tilapia also showed that dietary SA reduced the expression of pro-inflammatory factors (*IL-8*, *IL-12*, *TNF-α*, and *IL-1β*) by inhibiting MAPK and NF-κB signaling pathways (Li et al., 2020a). Additionally, dietary SB reduced the expression of pro-inflammatory factors (*TNF-α*, *IL-1β*, *IL-6*, and *IL-8*) through this signaling pathway and enhanced intestinal immune function in grass carp (Tian et al., 2017). In the present study, multiple experimental approaches consistently demonstrated that HC induced intestinal apoptosis, while dietary SA and SB reduced intestinal apoptosis by inhibiting the expression of pro-apoptotic genes (*bax*, *caspase3*, *caspase8*, and *caspase9*). The addition of SB to the HC diet of goats reduced the expression of pro-apoptotic genes (*caspase3, caspase8,* and *caspase9*) and inflammatory genes, which in turn inhibited the inflammatory response and reduced hepatocyte apoptosis (Chang et al., 2018). Studies in mice have also shown that SA inhibits cisplatin-induced apoptosis by attenuating the production of ROS (Zheng et al., 2023). Therefore, we suggest that this anti-apoptotic effect of SA and SB is retained in the intestine of the HC group.

A chronic HC diet causes ERS, leading to the disruption of lipid homeostasis that in turn leads to excessive intestinal lipid deposition, creating a vicious circle (Baiceanu et al., 2016; Kim et al., 2018; Zhang et al., 2021). ERS activates de novo adipogenesis by inducing the expression of SREBP-1c through the XBP-1 pathway (Lee et al., 2008). De novo adipogenesis suppresses fatty acid β-oxidation due to the adverse effect of the adipogenic intermediate malonyl-CoA on CPT1 activity (Morris et al., 2011). Thus, ERS promotes excessive lipid deposition primarily through induction of adipogenesis and inhibition of β-oxidation. In the current study, we observed abnormal accumulation of intestinal fat in the HC group; further studies suggested that this results from increased lipid synthesis pathways and inhibition of ectopic deposition due to catabolic pathways. However, we found that dietary SA and SB reduced HC-induced excess intestinal lipid deposition by inhibiting lipogenesis (*FAS*, *ACCA*, *SCD1*, and *PPARγ*) and activating lipolytic pathways (*CPT1α*, *HSL*, *AMPKα*, *PGC1α*, and *PPARα*) in the gut of largemouth bass. Similar studies have demonstrated that SA attenuates hepatic lipid deposition in Nile tilapia by activating lipolytic metabolism (Zhou et al., 2023). Studies on grass carp have shown that SB reduced hepatic lipid accumulation and improved organismal health (Zhou et al., 2019). Interestingly, dietary SB also improved abnormal lipid metabolism in mice fed a high-fat diet (Adeyanju et al., 2021). Thus, SA and SB play important roles in alleviating

lipid metabolism disorders caused by HC and high-fat diets, and the remission effect of SA is slightly better than that of SB.

5. Conclusions

In this study, we evaluated the efficacy and mechanisms of dietary SA and SB in reducing HC-induced intestinal damage in juvenile largemouth bass. We found that dietary SA and SB reduced intestinal inflammation and apoptosis, reduced intestinal damage, and repaired the intestinal barrier by inhibiting HC-induced ERS in juvenile largemouth bass. We further observed that dietary SA and SB inhibited lipogenesis and promoted lipolysis to reduce excessive intestinal fat deposition. These findings demonstrate that SA and SB are viable aquafeed additives that can protect the intestinal health of aquaculture animals.

Author contributions

Liulan Zhao: Funding acquisition, Project administration, Data curation, Conceptualization, Methodology. **Liangshun Cheng:** Software, Data curation, Formal analysis, Sample collection, Writing – original draft. **Yifang Hu:** Formal analysis, Investigation, Writing-original draft. **Xiaohui Li:** Methodology, Investigation. **Yihui Yang:** Methodology, Investigation. **Jin Mu:** Sample collection, Validation. **Lianfeng Shen:** Data curation. **Guojun Hu:** Writing – review & editing. **Kuo He:** Date analysis. **Haoxiao Yan:** Writing – review. **Qiao Liu:** Writing – review & editing. **Song Yang:** Project administration, Resources, Supervision, Writing – review & editing.

Declaration of competing interest

We declare that we have no financial and personal relationships with other people or organizations that can inappropriately influence our work, and there is no professional or other personal interest of any nature or kind in any product, service and/or company that could be construed as influencing the content of this paper.

Acknowledgments

This study was sponsored by Natural Science Foundation of Sichuan Province (2023NSFSC1220).

References

Abdel-Mohsen HH, Wassef EA, El-Bermawy NM, Abdel-Meguid NE, Saleh NE, Barakat KM, et al. Advantageous effects of dietary butyrate on growth, immunity response, intestinal microbiota and histomorphology of European Seabass (*Dicentrarchus labrax*) fry. Egypt J Aquat Biol Fish 2018;22(4):93–110.

Abdel-Tawwab M, Shukry M, Farrag FA, El-Shafai NM, Dawood MA, Abdel-Latif HM. Dietary sodium butyrate nanoparticles enhanced growth, digestive enzyme activities, intestinal histomorphometry, and transcription of growth-related genes in Nile tilapia juveniles. Aquaculture 2021;536:736467.

Adeyanju OA, Badejogbin OC, Areola DE, Olaniyi KS, Dibia C, Soetan OA, et al. Sodium butyrate arrests pancreato-hepatic synchronous uric acid and lipid dysmetabolism in high fat diet fed Wistar rats. Biomed Pharmacother 2021;133:110994.

Ali MZ, Jauncey K. Optimal dietary carbohydrate to lipid ratio in African catfish Clarias gariepinus (Burchell 1822). Aquac Int 2004;12:169–80.

AOAC. Official Methods of Analysis. 18th ed. Gaithersburg, MD: AOAC International; 2005.

Baiceanu A, Mesdom P, Lagouge M, Foufelle F. Endoplasmic reticulum proteostasis in hepatic steatosis. Nat Rev Endocrinol 2016;12(12):710–22.

Bibbò S, Ianiro G, Giorgio V, Scaldaferri F, Masucci L, Gasbarrini A, et al. The role of diet on gut microbiota composition. Eur Rev Med Pharmacol Sci 2016;20(22):4742–9.

Boshra H, Li J, Sunyer JO. Recent advances on the complement system of teleost fish. Fish Shellfish Immunol 2006;20(2):239–62.

Chang G, Liu X, Ma N, Yan J, Dai H, Roy AC, et al. Dietary addition of sodium butyrate contributes to attenuated feeding-induced hepatocyte apoptosis in dairy goats. J Agric Food Chem 2018;66(38):9995–10002.

Chen W, Gao S, Chang K, Zhao X, Niu B. Dietary sodium butyrate supplementation improves fish growth, intestinal microbiota composition, and liver health in largemouth bass (*Micropterus salmoides*) fed high-fat diets. Aquaculture 2023;564:739040.

Chen X, Kong Q, Zhao X, Zhao C, Hao P, Irshad I, et al. Sodium acetate/sodium butyrate alleviates lipopolysaccharide-induced diarrhea in mice via regulating the gut microbiota, inflammatory cytokines, antioxidant levels, and NLRP3/Caspase-1 signaling. Front Microbiol 2022;13.

Díez-Sainz E, Lorente-Cebrián S, Aranaz P, Riezu-Boj JI, Martínez JA, Milagro FI. Potential mechanisms linking food-derived microRNAs, gut microbiota and intestinal barrier functions in the context of nutrition and human health. Front Nutr 2021;8:586564.

Ding X, Yao L, Hou Y, Hou Y, Wang G, Fan J, et al. Effects of different carbohydrate levels in puffed feed on digestive tract morphological function and liver tissue structure of snakeheads (*Channa argus*). Aquac Res 2020;51(2):557–68.

Estensoro I, Ballester-Lozano G, Benedito-Palos L, Grammes F, Martos-Sitcha JA, Mydland L, et al. Dietary butyrate helps to restore the intestinal status of a marine teleost (*Sparus aurata*) fed extreme diets low in fish meal and fish oil. PLoS One 2016;11(11):e166564.

Fan Z, Wu D, Li J, Zhang Y, Cui Z, Li T, et al. Assessment of fish protein hydrolysates in juvenile largemouth bass (*Micropterus salmoides*) diets: effect on growth, intestinal antioxidant status, immunity, and microflora. Front Nutr 2022;9:109.

Fang W, Chen Q, Li J, Liu Y, Zhao Z, Shen Y, et al. Endoplasmic reticulum stress disturbs lipid homeostasis and augments inflammation in the intestine and isolated intestinal cells of Large yellow croaker (*Larimichthys crocea*). Front Immunol 2021;12:738143.

Feng J, Cui W, Liu S, Liu X, Cai Z, Chang X, et al. Dietary sodium acetate (SA) improves the growth performance, intestinal health, and carbohydrate metabolism of juvenile common carp (*Cyprinus carpio*). Aquac Rep 2022a;27:101350.

Feng Z, Zhong Y, He G, Sun H, Chen Y, Zhou W, et al. Yeast culture improved the growth performance, liver function, intestinal barrier and microbiota of juvenile largemouth bass (*Micropterus salmoides*) fed high-starch diet. Fish Shellfish Immunol 2022b;120:706–15.

Fu Y, Wang B, Zhang Q, Xu D, Lin D, Yang X, et al. Combined effects of Chinese medicine feed and ginger extract bath on co-infection of Ichthyophthirius multifiliis and Dactylogyrus ctenopharyngodonid in grass carp. Parasitol Res 2017;116:2017–25.

Hu Y, Liu J, Yuan Y, Chen J, Cheng S, Wang H, et al. Sodium butyrate mitigates type 2 diabetes by inhibiting PERK-CHOP pathway of endoplasmic reticulum stress. Environ Toxicol Pharmacol 2018;64:112–21.

Huang X, Zhong L, Kang Q, Liu S, Feng Y, Geng Y, et al. A high starch diet alters the composition of the intestinal microbiota of largemouth bass micropterus salmoides, which may be associated with the development of enteritis. Front Microbiol 2021;12:696588.

Huang Y, Wang Y, Feng Y, Wang P, He X, Ren H, et al. Role of endoplasmic reticulum stress-autophagy axis in severe burn-induced intestinal tight junction barrier dysfunction in mice. Front Physiol 2019;10:606.

Jia R, Cao L, Du J, He Q, Gu Z, Jeney G, et al. Effects of high-fat diet on steatosis, endoplasmic reticulum stress and autophagy in liver of tilapia (*Oreochromis niloticus*). Front Mar Sci 2020;7:363.

Kim JY, Garcia-Carbonell R, Yamachika S, Zhao P, Dhar D, Loomba R, et al. ER stress drives lipogenesis and steatohepatitis via caspase-2 activation of S1P. Cell 2018;175(1):133–45.

Kumar S, Sahu NP, Pal AK, Choudhury D, Yengkokpam S, Mukherjee SC. Effect of dietary carbohydrate on haematology, respiratory burst activity and histological changes in L. rohita juveniles. Fish Shellfish Immunol 2005;19(4):331–44.

Lee A, Scapa EF, Cohen DE, Glimcher LH. Regulation of hepatic lipogenesis by the transcription factor XBP1. Science 2008;320(5882):1492–6.

Li M, Hu F, Qiao F, Du Z, Zhang M. Sodium acetate alleviated high-carbohydrate induced intestinal inflammation by suppressing MAPK and NF-κB signaling pathways in Nile tilapia (*Oreochromis niloticus*). Fish Shellfish Immunol 2020a;98:758–65.

Li S, Heng X, Guo L, Lessing DJ, Chu W. SCFAs improve disease resistance via modulate gut microbiota, enhance immune response and increase antioxidative capacity in the host. Fish Shellfish Immunol 2022b;120:560–8.

Li X, Zheng S, Ma X, Cheng K, Wu G. Effects of dietary starch and lipid levels on the protein retention and growth of largemouth bass (*Micropterus salmoides*). Amino Acids 2020c;52(6–7):999–1016.

Liang X, Chen P, Wu X, Xing S, Morais S, He M, et al. Effects of high starch and supplementation of an olive extract on the growth performance, hepatic antioxidant capacity and lipid metabolism of largemouth bass (*Micropterus salmoides*). Antioxidants 2022;11(3):577.

Lin S, Shi C, Mu M, Chen Y, Luo L. Effect of high dietary starch levels on growth, hepatic glucose metabolism, oxidative status and immune response of juvenile largemouth bass, *Micropterus salmoides*. Fish Shellfish Immunol 2018;78:121–6.

McCarville JL, Chen GY, Cuevas VD, Troha K, Ayres JS. Microbiota metabolites in health and disease. Annu Rev Immunol 2020;38:147–70.

Medzhitov R. Origin and physiological roles of inflammation. Nature 2008;454(7203):428–35.

Morris EM, Rector RS, Thyfault JP, Ibdah JA. Mitochondria and redox signaling in steatohepatitis. 2011.

Oshima T, Miwa H, Joh T. Changes in the expression of claudins in active ulcerative colitis. J Gastroenterol Hepatol 2008;23:S146–50.

Pan M, Liu D, Liu J, Li X, Huang D, Luo K, et al. Biotin alleviates hepatic and intestinal inflammation and apoptosis induced by high dietary carbohydrate in juvenile turbot (*Scophthalmus maximus L.*). Fish Shellfish Immunol 2022;130:560–71.
Park J, Kim M, Kang SG, Jannasch AH, Cooper B, Patterson J, et al. Short-chain fatty acids induce both effector and regulatory T cells by suppression of histone deacetylases and regulation of the mTOR–S6K pathway. Mucosal Immunol 2015;8(1):80–93.
Robles R, Lozano AB, Sevilla A, Márquez L, Nuez-Ortín W, Moyano FJ. Effect of partially protected butyrate used as feed additive on growth and intestinal metabolism in sea bream (*Sparus aurata*). Fish Physiol Biochem 2013;39: 1567–80.
Sankian Z, Khosravi S, Kim Y, Lee S. Effect of dietary protein and lipid level on growth, feed utilization, and muscle composition in golden Mandarin fish *Siniperca scherzeri*. Fish Aquat Sci 2017;20:1–6.
Sano R, Reed JC. ER stress-induced cell death mechanisms. Biochim Biophys Acta 2013;1833(12):3460–70.
Shi Y, Zhong L, Fan Y, Zhang J, Zhong H, Liu X, et al. The protective effect of mulberry leaf flavonoids on high-carbohydrate-induced liver oxidative stress, inflammatory response and intestinal microbiota disturbance in *Monopterus albus*. Antioxidants 2022a;11(5):976.
Shi Y, Zhong L, Zhong H, Zhang J, Liu X, Peng M, et al. Taurine supplements in high-carbohydrate diets increase growth performance of *Monopterus albus* by improving carbohydrate and lipid metabolism, reducing liver damage, and regulating intestinal microbiota. Aquaculture 2022b;554:738150.
Song X, Qiao L, Chang J, Dou X, Zhang X, Pi S, et al. Dietary supplementation with selenium nanoparticles-enriched Lactobacillus casei ATCC 393 alleviates intestinal barrier dysfunction of mice exposed to deoxynivalenol by regulating endoplasmic reticulum stress and gut microbiota. Ecotoxicol Environ Saf 2022;248:114276.
Suzuki T. Regulation of intestinal epithelial permeability by tight junctions. Cell Mol Life Sci 2013;70:631–59.
Tian L, Zhou X, Jiang W, Liu Y, Wu P, Jiang J, et al. Sodium butyrate improved intestinal immune function associated with NF-κB and p38MAPK signalling pathways in young grass carp (*Ctenopharyngodon idella*). Fish Shellfish Immunol 2017;66:548–63.
Wan ML, Ling KH, El-Nezami H, Wang MF. Influence of functional food components on gut health. Crit Rev Food Sci Nutr 2019;59(12):1927–36.
Wang Q, Cheng L, Liu J, Li Z, Xie S, De Silva SS. Freshwater aquaculture in PR C hina: trends and prospects. Rev Aquac 2015;7(4):283–302.
Wang T, Wu H, Li W, Xu R, Qiao F, Du Z, et al. Effects of dietary mannan oligosaccharides (MOS) supplementation on metabolism, inflammatory response and gut microbiota of juvenile Nile tilapia (*Oreochromis niloticus*) fed with high carbohydrate diet. Fish Shellfish Immunol 2022;130:550–9.
Wang T, Zhang N, Yu X, Qiao F, Chen L, Du Z, et al. Inulin alleviates adverse metabolic syndrome and regulates intestinal microbiota composition in Nile tilapia (*Oreochromis niloticus*) fed with high-carbohydrate diet. Br J Nutr 2021;126(2):161–71.
Wu L, Xu Y, Hogstrand C, Zhao T, Wu K, Xu Y, et al. Lipophagy mediated glucose-induced changes of lipid deposition and metabolism via ROS dependent AKT-Beclin1 activation. J Nutr Biochem 2022;100:108882.
Wu P, Tian LI, Zhou X, Jiang W, Liu Y, Jiang J, et al. Sodium butyrate enhanced physical barrier function referring to Nrf2, JNK and MLCK signaling pathways in the intestine of young grass carp (*Ctenopharyngodon idella*). Fish Shellfish Immunol 2018;73:121–32.
Wu Z, Niu J, Xue H, Wang S, Zhao P. Sodium 4-phenylbutyrate protects hypoxic-ischemic brain injury via attenuating endoplasmic reticulum stress in neonatal rats. Front Behav Neurosci 2021;15:632143.
Xie D, Yang L, Yu R, Chen F, Lu R, Qin C, et al. Effects of dietary carbohydrate and lipid levels on growth and hepatic lipid deposition of juvenile tilapia, *Oreochromis niloticus*. Aquaculture 2017;479:696–703.
Xu R, Li M, Wang T, Zhao Y, Shan C, Qiao F, et al. Bacillus amyloliquefaciens ameliorates high-carbohydrate diet-induced metabolic phenotypes by restoration of intestinal acetate-producing bacteria in Nile Tilapia. Br J Nutr 2022;127(5): 653–65.
Xun P, Zhou C, Huang X, Huang Z, Yu W, Yang Y, et al. Effects of dietary sodium acetate on intestinal health of juvenile *Trachinotus ovatus* based on multi-omics approach. Aquaculture 2023;562:738776.
Zhang H, Ding Q, Wang A, Liu Y, Teame T, Ran C, et al. Effects of dietary sodium acetate on food intake, weight gain, intestinal digestive enzyme activities, energy metabolism and gut microbiota in cultured fish: zebrafish as a model. Aquaculture 2020;523:735188.
Zhang J, Yi M, Zha L, Chen S, Li Z, Li C, et al. Sodium butyrate induces endoplasmic reticulum stress and autophagy in colorectal cells: implications for apoptosis. PLoS One 2016;11(1):e147218.
Zhang Y, Chen H, Zhu W, Yu K. Cecal infusion of sodium propionate promotes intestinal development and jejunal barrier function in growing pigs. Animals 2019;9(6):284.
Zhang Y, Liu Y, Ma H, Sun M, Wang X, Jin S, et al. Insufficient or excessive dietary carbohydrates affect gut health through change in gut microbiota and regulation of gene expression of gut epithelial cells in grass carp (*Ctenopharyngodon idella*). Fish Shellfish Immunol 2023;132:108442.
Zhang Y, Wei Z, Yang M, Liu D, Pan M, Wu C, et al. Dietary taurine modulates hepatic oxidative status, ER stress and inflammation in juvenile turbot (*Scophthalmus maximus L.*) fed high carbohydrate diets. Fish Shellfish Immunol 2021;109:1–11.
Zhao H, Peng K, Wang G, Mo W, Huang Y, Cao J. Metabolic changes, antioxidant status, immune response and resistance to ammonia stress in juvenile yellow catfish (*Pelteobagrus fulvidraco*) fed diet supplemented with sodium butyrate. Aquaculture 2021a;536:736441.
Zhao H, Wang G, Wang H, Mo W, Huang Y, Cao J, et al. Effects of dietary sodium butyrate on growth, digestive enzymes, body composition and nutrient retention-related gene expression of juvenile yellow catfish (*Pelteobagrus fulvidraco*). Anim Nutr 2021b;7(2):539–47.
Zhao L, Liang J, Chen F, Tang X, Liao L, Liu Q, et al. High carbohydrate diet induced endoplasmic reticulum stress and oxidative stress, promoted inflammation and apoptosis, impaired intestinal barrier of juvenile largemouth bass (*Micropterus salmoides*). Fish Shellfish Immunol 2021c;119:308–17.
Zhao L, Liang J, Liu H, Gong C, Huang X, Hu Y, et al. Yinchenhao Decoction ameliorates the high-carbohydrate diet induced suppression of immune response in largemouth bass (*Micropterus salmoides*). Fish Shellfish Immunol 2022;125: 141–51.
Zhao L, Liao L, Tang X, Liang J, Liu Q, Luo W, et al. High-carbohydrate diet altered conversion of metabolites, and deteriorated health in juvenile largemouth bass. Aquaculture 2022;549:737816.
Zhao L, Tang G, Xiong C, Han S, Yang C, He K, et al. Chronic chlorpyrifos exposure induces oxidative stress, apoptosis and immune dysfunction in largemouth bass (*Micropterus salmoides*). Environ Pollut 2021d;282:117010.
Zhao T, Wu K, Hogstrand C, Xu Y, Chen G, Wei C, et al. Lipophagy mediated carbohydrate-induced changes of lipid metabolism via oxidative stress, endoplasmic reticulum (ER) stress and ChREBP/PPARγ pathways. Cell Mol Life Sci 2020b;77:1987–2003.
Zhao T, Yang S, Chen G, Xu Y, Xu Y, Luo Z. Dietary glucose increases glucose absorption and lipid deposition via SGLT1/2 signaling and acetylated ChREBP in the intestine and isolated intestinal epithelial cells of yellow catfish. J Nutr 2020a;150(7):1790–8.
Zheng J, Wang S, Tang S, Hsin I, Kang Y, Hsu C, et al. Sodium acetate ameliorates cisplatin-induced kidney injury in vitro and in vivo. Chem Biol Interact 2023;369:110258.
Zhou C, Liu B, Ge X, Xie J, Xu P. Effect of dietary carbohydrate on the growth performance, immune response, hepatic antioxidant abilities and heat shock protein 70 expression of Wuchang bream, *Megalobrama amblycephala*. J Appl Ichthyol 2013;29(6):1348–56.
Zhou JS, Guo P, Yu HB, Ji H, Lai ZW, Chen YA. Growth performance, lipid metabolism, and health status of grass carp (*Ctenopharyngodon idella*) fed three different forms of sodium butyrate. Fish Physiol Biochem 2019;45:287–98.
Zhou W, Limbu SM, Li R, Luo Y, Ren J, Qiao F, et al. Dietary sodium acetate improves high-fat diet utilization through promoting differential nutrients metabolism between liver and muscle in Nile tilapia (*Oreochromis niloticus*). Aquaculture 2023;565:739142.
Zhou Y, He G, Jin T, Chen Y, Dai F, Luo L, et al. High dietary starch impairs intestinal health and microbiota of largemouth bass, *Micropterus salmoides*. Aquaculture 2021;534:736261.
Zou X, Ji J, Qu H, Wang J, Shu DM, Wang Y, et al. Effects of sodium butyrate on intestinal health and gut microbiota composition during intestinal inflammation progression in broilers. Poultry Sci 2019;98(10):4449–56.